First Results from the XXL Survey and Associated Multi-wavelength Programmes

Christophe Adami[1]
Marguerite Pierre[2]
Nikola Baran[3]
Dominique Eckert[4]
Sotiria Fotopoulou[4]
Paul A. Giles[5]
Elias Koulouridis[2]
Chris Lidman[6]
Maggie Lieu[7]
Adam B. Mantz[8]
Florian Pacaud[9]
Emanuela Pompei[10]
Vernesa Smolčić[3]
Felicia Ziparo[8]
and the XXL Team[11]

[1] Aix Marseille Université, CNRS, LAM UMR 7326, Marseille, France
[2] Laboratoire AIM, CEA/DSM/IRFU/SAp, CEA Saclay, Gif-sur-Yvette, France
[3] Department of Physics, University of Zagreb, Croatia
[4] Department of Astronomy, University of Geneva, Versoix, Switzerland
[5] H. H. Wills Physics Laboratory, University of Bristol, United Kingdom
[6] Australian Astronomical Observatory, North Ryde, Australia
[7] School of Physics & Astronomy, University of Birmingham, United Kingdom
[8] Department of Astronomy and Astrophysics, University of Chicago, USA
[9] Argelander Institut für Astronomie, Universität Bonn, Germany
[10] ESO
[11] XXL Team: http://irfu.cea.fr/xxl/members

The XXL survey has mapped two extragalactic regions of 25 square degrees, using 10 ks XMM observations down to a point source sensitivity of ~ 5 × 10^{-15} erg s^{-1} cm^{-2} in the 0.5–2 keV band. It is the largest XMM project approved to date (> 6 Ms in total). The two fields have been or will be observed by several ground- and space-based facilities from ultra-violet to radio wavelengths. Besides the imaging, the spectroscopic follow-up is of special interest and ESO has contributed through Large Programmes and dedicated allocations. As of December 2015, ~ 450 new galaxy clusters are detected to z ~ 1.5–2, as well as more than 22 000 active galactic nuclei (AGN) to z ~ 4. The main goal of the project is to constrain the dark energy equation of state using clusters of galaxies. This survey will have lasting legacy value for cluster scaling laws and studies of AGNs and the X-ray background. The first XXL scientific results are summarised.

Introduction

The distribution of matter in the Universe reveals its history: small density perturbations present at the time of recombination (just after the Cosmic Microwave Background [CMB] was emitted) grew under the competing actions of gravity and expansion of spacetime. This led to the progressive formation of a remarkable network of filaments, sheets and voids that was first revealed from the galaxy distribution some 30 years ago and is now well rendered by numerical simulations. Basically as time proceeds, overdensities become denser and low density regions emptier as matter flows along the filaments. The rate at which structure forms and how it will ultimately develop is described by general relativity, depending on a set of cosmological parameters and on the nature of dark matter and dark energy (the latter being responsible for the acceleration of the expansion).

Tracking the evolution of cosmic structure in the quest for the cosmological parameters that describe the Universe is especially interesting, in particular to corroborate the cosmological constraints inferred from the CMB (z ~ 1000) and from the matter distribution at much later times (z ~ 0–4), since they originate from very different physical processes. A traditional approach follows the distribution of galaxies in visible or infrared light. However galaxies account only for a few percent of the total matter content and are highly nonlinear objects, which makes establishing the connection with the initial density spectrum non-trivial. At the upper hierarchical level, one finds clusters of galaxies, the most massive objects in the Universe. They are located at the nodes of the cosmic web and are huge reservoirs of hot gas that fill the space between the galaxies. The gas has a temperature of a few tens of millions of degrees and emits in the X-ray.

The cosmological analysis of cluster surveys basically relies on number counts (*dn/dz* or *dn/dM/dz*) and on the spatial analysis (3D correlation function). In order to establish these functions, it is necessary to have a good knowledge of: (i) the scaling relations that link the X-ray observables, like temperature and luminosity, to the mass; and (ii) the selection function, i.e., the probability of detecting a cluster of given mass as a function of redshift.

In this context, the XXL project (XXL Paper I) has undertaken a large survey of the X-ray sky with the European Space Agency XMM-Newton observatory. The primary goal of the XXL survey is to detect and confirm a few hundred clusters back to a time when the age of Universe was about half of its present value, i.e., z ~ 1. From this data collection, we can infer the evolutionary properties and spatial distribution of the deepest potential wells of the Universe and, subsequently, test various cosmological scenarios. In addition, XXL will deliver several tens of thousands of active galactic nuclei (AGNs) out to a redshift of at least four, allowing statistical studies of the AGN population as a function of environment to be performed.

The XXL Survey is an XMM Very Large Programme that covers two extragalactic areas of 25 square degrees, located around (RA, Dec) of (2h 20m, −4.5°) and (23h 30m, −55°). Over 500 XMM XXL observations, typically of 10 ks each, were performed between 2011 and 2013. Two years after the completion of the X-ray observations, we have detected ~ 450 clusters and 22 000 AGNs in the 0.5–2.0 keV energy band. The XXL survey samples the low end of the cluster mass function around z ~ 0.3–0.5. This group population is especially interesting, since it contains the building blocks of the local massive clusters. Moreover, it is sensitive to non-gravitational physics, like the energy input from AGNs, feedback from star formation or cooling processes. Such groups thus present useful environments in which to study the formation of cosmic structures and provide a unique input to test physical processes via numerical simulations. The XXL consortium gathers some 100 scientists including observers, theoreticians and simulators with a wide range of expertise encompassing the entire electromagnetic spectrum.

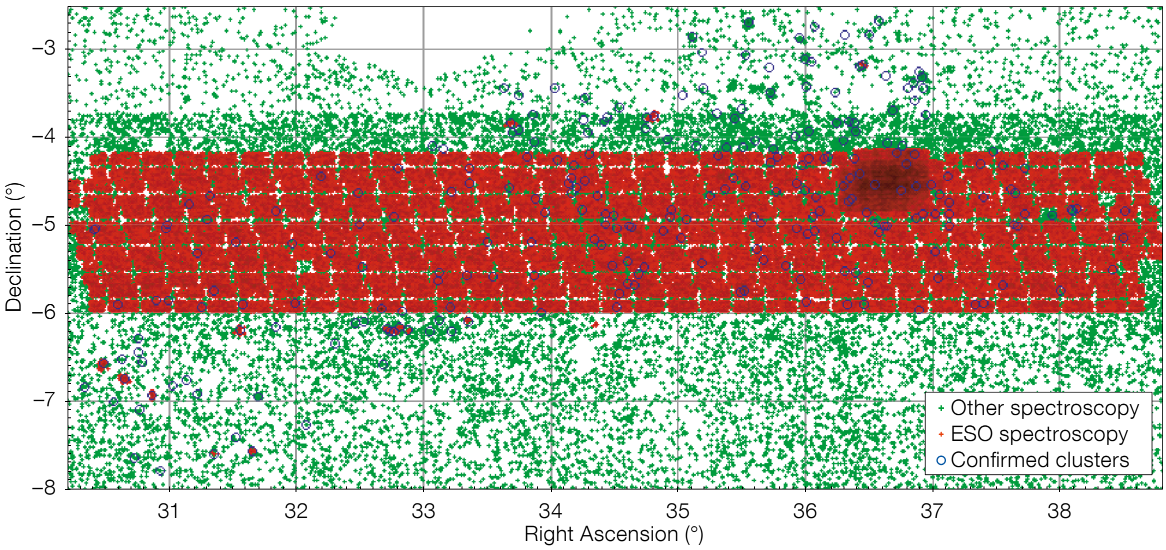

Figure 1. Sky distribution of the available spectroscopy and confirmed X-ray clusters of galaxies in the northern XXL field. The chessboard pattern of red points corresponds to the mosaic of VIMOS fields from the VIPERS survey (Guzzo et al., 2014), while the darker spot at RA = 36.5 degrees shows the deeper data from the VIMOS-VLT Deep Survey (VVDS; Le Fèvre et al., 2005). The isolated concentrations of red points are from the XXL ESO Large Programme (191.A-0268) and represent ~ 50 % of the redshifts inside all the confirmed clusters at $z > 0.5$.

Associated multi-wavelength programmes and XXL samples

In order to characterise the properties of the detected clusters and AGNs, the XXL survey is accompanied by a comprehensive follow-up programme. Observations are coordinated with the largest ground-based and space observatories, from the X-ray to the radio (see, for example, XXL paper X for the *K*-band luminosity–weak-lensing mass relation for galaxy structures). Of these coordinated observations, the ESO Large Programme and principal investigator allocations (ESO 191.A-0268, 089.A-0666, and 60.A-9302), as well as galaxy surveys in the XXL fields, like the VIMOS Public Extragalactic Survey (VIPERS; for example, Guzzo et al., 2014) and the Galaxy And Mass Assembly survey (GAMA; for example, Driver et al., 2016), are of special relevance as they allow galaxy redshifts to be measured, hence accurately locating the galaxy clusters in 3D space (Figures 1 and 2). In the framework of the ESO Large Programme, we observed clusters out to a redshift of ~ 0.5 at the New Technology Telescope (NTT) with the ESO Faint Object Spectrograph and Camera 2 (EFOSC2) and the more distant ones ($0.5 < z < 1.2$) with the FOcal Reducer/low dispersion Spectrograph 2 (FORS2) instrument on the Very Large Telescope (VLT). An example from the latter is the detection of a $z \sim 1.9$ cluster (see XXL Paper V).

Cluster redshifts constitute a critical input to cosmological analysis, allowing the computation of the cluster–cluster correlation function and further topological studies. Detailed investigations of the dynamics and galaxy properties of individual clusters are also undertaken at the William Herschel Telescope (WHT). The redshift measurement of the AGN is systematically performed with the AAOmega instrument on the Australian Astronomical Telescope (XXL XIV). Radio follow-up of the X-ray AGNs is undertaken with Giant Meterwave Radio Telescope (GMRT), the Jansky Very Large Array (VLA) and the Australia Telescope Compact Array (ATCA). In parallel, four numerical simulation programmes provide the necessary material to test *in situ* the various physical mechanisms that drive cluster and AGN evolution and their respective interactions. Simulations also allow accurate determination of the cluster selection function, which is an essential ingredient for the cosmological analysis.

In a first series of 13 articles published in the December 2015 *Astronomy & Astrophysics* special issue, plus one in *Publications of the Astronomical Society of Australia*, we released the catalogues of the brightest 100 clusters (XXL-100-GC) and 1000 AGNs (XXL-1000-AGN) as well as the reduced XMM observations. We present a number of scientific results for the, to date, little-explored low-mass range characterising the XXL cluster sample.

Scaling relations

Scaling relations are key elements for parameterising cluster evolution and the XXL project aims at a self-consistent determination. We therefore investigated the luminosity–temperature (LT) relation of the XXL-100-GC sample (XXL III, see also XXL IV for the mass–temperature relation). The first step was to measure the cluster X-ray luminosity and temperature from the XMM survey data. The sample spans a wide range of redshift ($0.05 < z < 1.05$), temperature ($0.6 < kT < 7.0$ keV), and luminosity ($9 \times 10^{41} < L < 5 \times 10^{43}$ erg s^{-1}) and is equivalent to a flux-limited sample (3×10^{-14} erg s^{-1} cm^{-2}).

Our methods to determine the LT relation fully take into account the selection effects of the survey. We measure the evolution of the LT relation internally using the broad redshift range of the sample and find a slope of the bolometric LT relation that is steeper than the self-similar expectation. Regarding evolution, our best fit is fully consistent with strong self-similar evolution where clusters scale self-similarly with both mass and redshift: clusters in the past would appear as scaled replicates of the local ones, as a function of mass. However, this result is marginally more significant than the weak self-similar evolution solution, where clusters scale with redshift alone. We further investigated the sensitivity of our results to the assumptions made in our fitting model, finding that the use of an external LT relation as a low-*z* baseline can have a profound effect on the measured evolution. The present calculations were performed assuming a given cosmology. The next step, involving the complete XXL sample, will be to implement the cosmological dependency of the luminosity in the determination of the evolution rate of the LT relation.

Cosmological constraints

We further used the XXL-100-GC sample to infer preliminary cosmological constraints (XXL II). The measured luminosities and temperatures allowed us to model the predicted cluster number counts for the presently favoured set of cosmological parameters. The number density of clusters is found to be less than predicted by the Planck CMB cosmology, once the XXL selection effects are duly accounted for; this tension is similar to that found for the Planck Sunyaev–Zeldovich (S–Z) detected cluster sample, but pertains to a cluster mass range about one order of magnitude lower. However, the alternate Nine Year Wilkinson Microwave Anisotropy Probe (WMAP9) model is not perfect either and still overpredicts the number of faint clusters. Basic attempts to assess the cosmological leverage of the sample revealed that, even with the current subsample, the error budget is already dominated by uncertainties in the cluster mass calibration, which therefore will be one of the priorities of the XXL cluster science programme over the next few years. In particular, we are starting a collaboration with the Subaru Hyper-SuprimeCam team in order to obtain reliable lensing masses for most of the XXL clusters.

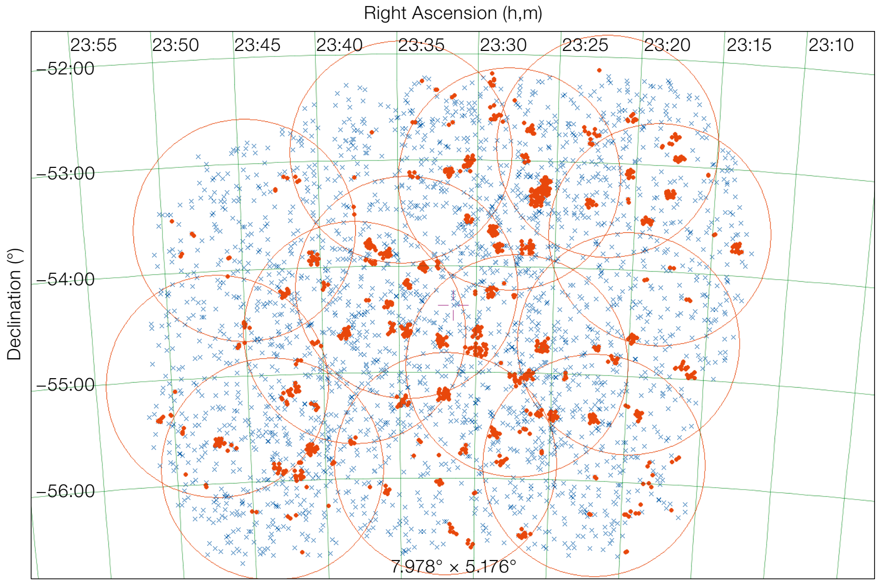

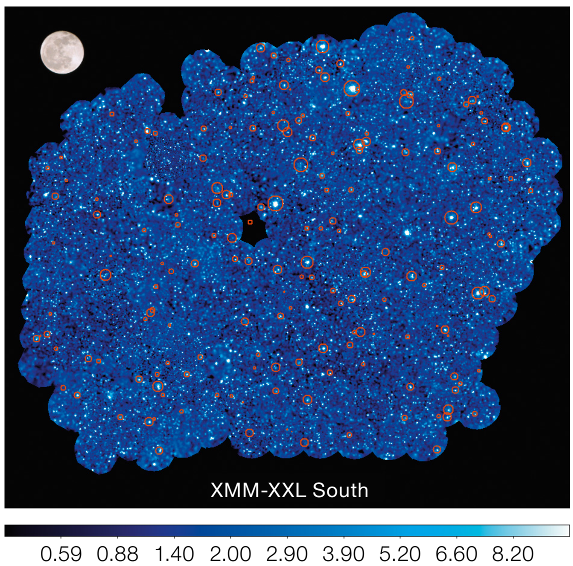

Figure 2. Upper: Spectroscopically confirmed AGNs (blue) and cluster galaxies (red) in the southern XXL field from the AAOmega follow-up (XXL Paper XIV). Left: Corresponding X-ray mosaic (units of colour bar are counts s^{-1} $degree^{-1}$). The 25-square-degree field is covered by some 220 XMM pointings. The XMM field of view has a size comparable to that of the Moon (30 arcminutes diameter, shown at the upper left). More than 12 000 AGNs have been detected in this image. The red circles show the clusters of galaxies.

Cluster baryon content

Beside counts and topology, another potential cosmological probe is the baryon fraction (f_{gas}) in clusters (XXL XIII). This test assumes that f_{gas} is constant as a function of redshift for the high-mass clusters, because they are supposed to have retained all the material accreted since their formation epoch. Gas mass and total mass measurements do not scale in the same way as a function of cosmology; therefore, requiring that their ratio is constant ought to put constraints on the cosmological parameters. We measured the number of baryons (X-ray gas and stars) in the XXL-100-GC sample. Halo masses were estimated from a mass–temperature relation that was directly calibrated using weak-lensing measurements (from the Canada France Hawaii Telescope Legacy Survey, CFHTLS) for a subset of XXL clusters. We find that the weak-lensing calibrated gas fraction of XXL-100-GC clusters is lower than was found in previous studies using hydrostatic masses.

We compared our f_{gas}–M relation with the predictions of cosmological simulations using different gas physics. It was found that our results favour extreme AGN feedback schemes in which a large fraction of the baryons are expelled from the potential well of dark matter halos. Such models are, however, in tension with X-ray-only proxies, such as the gas density and entropy profiles (Le Brun et al., 2014) and are not able to reproduce the relation between gas mass and temperature of XXL clusters.

Therefore, the results presented are challenging for current numerical simulations, and reconciling the observed gas fraction with the predictions would require that our weak-lensing masses be systematically overestimated. A mass

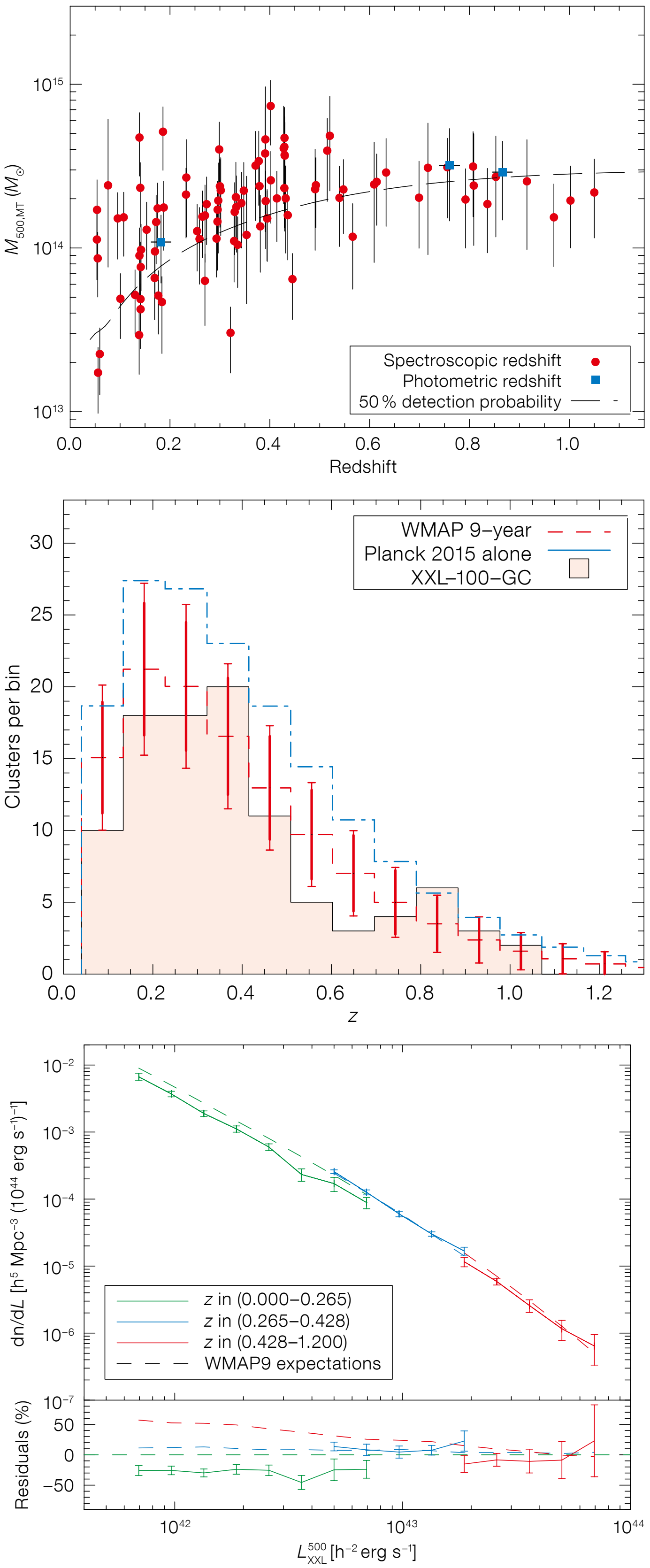

Figure 3. Upper: Distribution of the bright XXL cluster sample in the M_{500} vs. redshift plane. The dashed line shows the 50 % completeness limit in the WMAP9 cosmology. Middle: Redshift distribution of the XXL-100-GC sample (filled histogram) compared with different model expectations (CMB measurements from WMAP + H0 + BAO presented in Hinshaw et al. [2013], and latest CMB measurements from the Planck satellite, but without additional constraints from Planck Collaboration 2015). Lower: Differential luminosity function of the bright XXL cluster sample in three redshift bins. The lower plot shows the residuals with respect to the low-redshift WMAP9 prediction (XXL Paper II).

bias $1 - b = 0.58 \pm 0.04$, which is required to reconcile Planck cluster counts with the primary CMB, would further exacerbate the tension between the baryon fraction and the cosmological value, challenging our understanding of cluster physics. Therefore, a satisfactory solution to the tension between CMB and cluster counts must also simultaneously explain the low baryon fraction measured for the XXL halos.

Discovery of five superclusters

Given its depth and sky coverage, XXL is particularly suited to systematically unveiling the clustering of X-ray clusters and to identifying superstructures in a homogeneous X-ray sample down to the typical mass scale of a local massive cluster. Although a few isolated, very high redshift superclusters are known, our work is the first attempt to systematically unveil superstructures up to $z \sim 0.5$ in a homogeneous X-ray sample. In this framework, we discovered five low-mass superclusters consisting of three to seven galaxy structures.

One of them is particularly interesting and is presented in more detail (XXL VII and Figure 4). It is composed of six clusters of galaxies and the structure is very compact with all the clusters residing in one XMM pointing. Our subsequent spectroscopic follow-up with WHT and NTT provided a median redshift of $z \sim 0.43$. An estimate of the X-ray mass and luminosity of this supercluster returns values of 1.7×10^{15} $M_\odot$ and of 1.68×10^{44} erg s^{-1}, respectively, and a total gas mass of $M_{gas} = 9.3 \times 10^{13}$ $M_\odot$. Instead of having a massive central cluster with infalling filaments and smaller structures, it has almost two equal-sized objects, making it qualitatively different from the network around an already formed massive cluster. This supercluster is currently the most massive and most distant found in XXL. If we put together the relatively small crossing time, the common X-ray emission of three members, and the measured gas fraction and mass, we can speculate that we are observing an unrelaxed structure with an ongoing merging between at least three of the member clusters. If nothing else intervened to alter the system, and assuming that the estimated

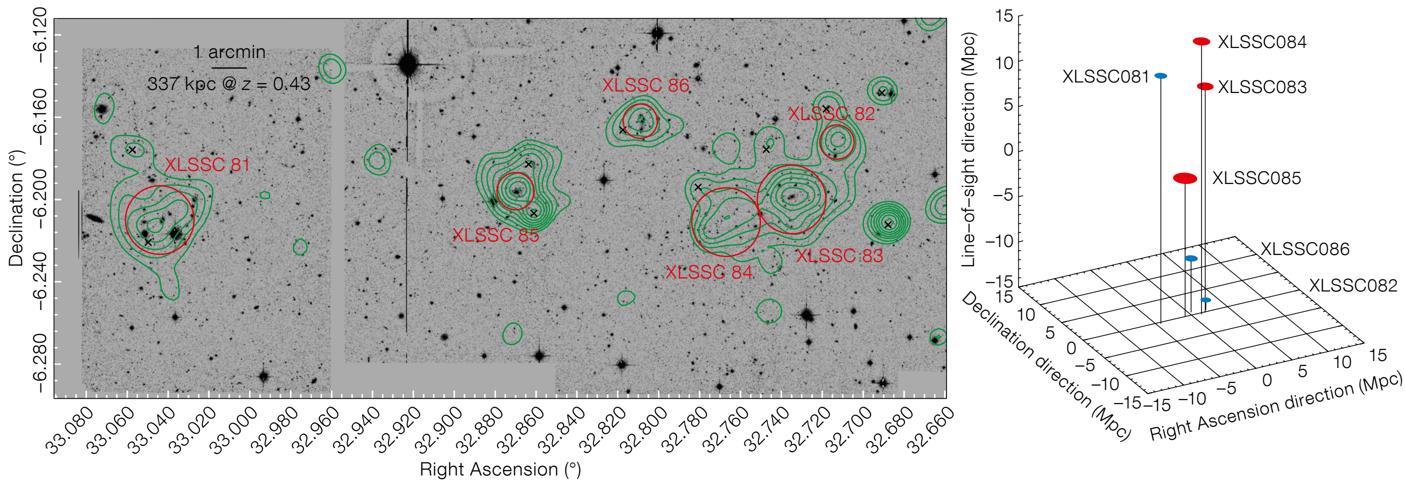

Figure 4. Top left: CFHTLS MegaCam mosaic image in the *i*-band with the XXL contours superimposed in green; X-ray clusters are red circles. The positions of the BCG in each cluster are shown and the black crosses highlight the point sources excluded from the X-ray analysis. Top right: Three-dimensional configuration of the $z = 0.43$ supercluster (XXL Paper VII). Right: CFHTLS-wide colour $u^*r'z'$ image (8 by 8 arcminutes) of XLSS-C 82-83-84 inner complex.

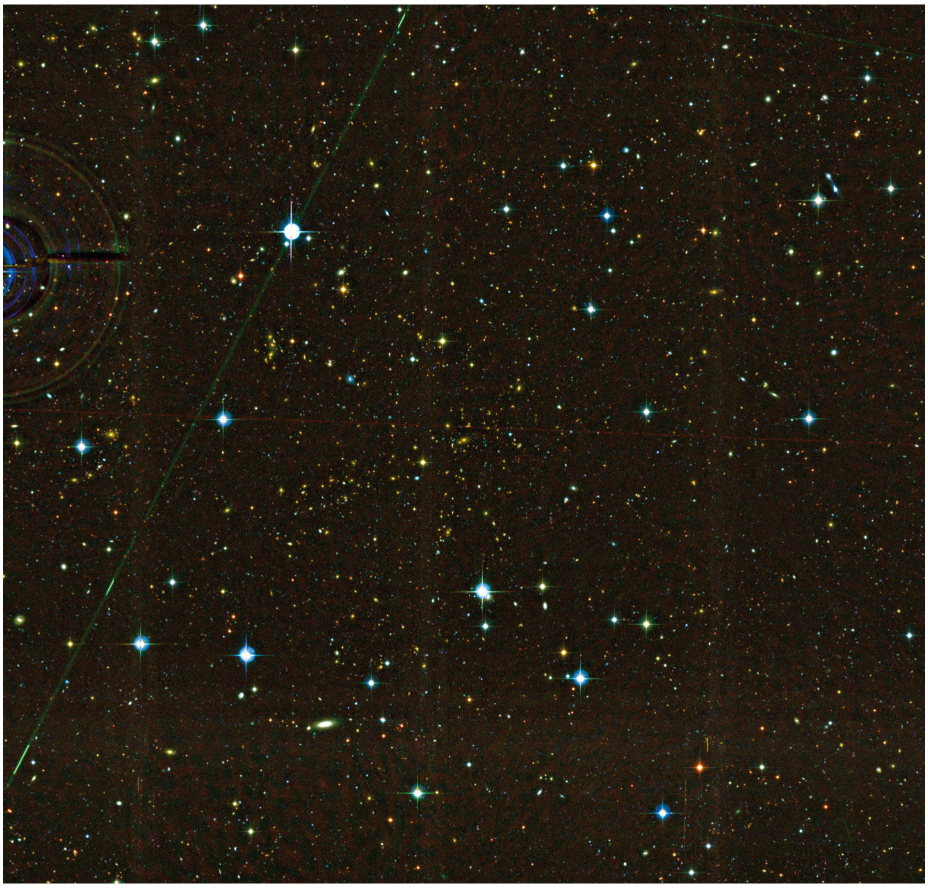

crossing time is a good estimate of the merging time, it is likely that by the present time the supercluster would already have completely merged ~ 2 Gyr before and resemble the most massive known clusters.

First spectral characterisation of diffuse light in a cluster

Within a cluster, gravitational effects can lead to the removal of stars from their parent galaxies and subsequent dispersal into the intracluster medium (ICL). Gas hydrodynamical effects can additionally strip gas and dust from galaxies. The properties of the ICL can therefore help constrain the physical processes at work in clusters by serving as a fossil record of the interaction history. We detected in the XXL survey a very peculiar intermediate-mass cluster: XLSSC-116, with a very high level of such diffuse light, by applying a wavelet-based method to CFHT Megacam and Wide-field InfraRed Camera (WIRCAM) images (XXL VIII). The amount of diffuse light is equivalent to two brightest cluster galaxies (BCGs) in the i'-band. To the best of our knowledge, this is the first detected cluster with such a large amount of diffuse light.

The source of the diffuse light was then spectroscopically characterised with ESO Multi-Unit Spectroscopic Explorer (MUSE) spectroscopic data (proposal 60.A-9302). MUSE data were also used to compute redshifts of 24 cluster galaxies and search for cluster substructures. The cluster consists of a main component with a velocity dispersion of the order of 600 km s^{-1} and an infalling low-mass group with a velocity dispersion of 170 km s^{-1}. Part of the detected diffuse light has a very weak optical stellar component and apparently consists mainly of gas emission, while other diffuse light sources are clearly dominated by old stars. Furthermore, emission lines were detected in several places coinciding with

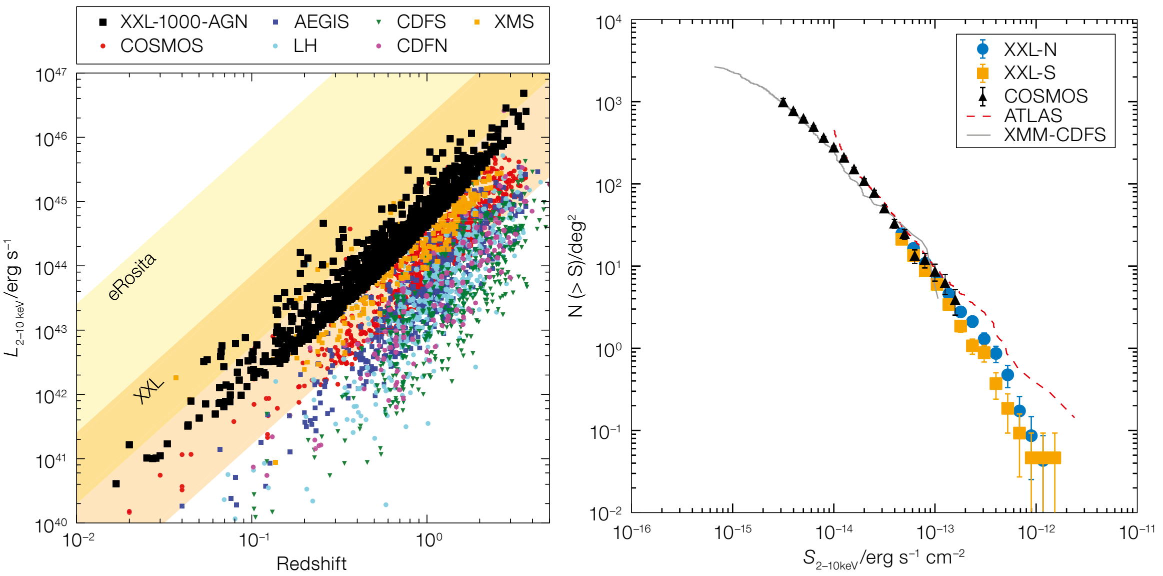

Figure 5. Left: Luminosity–redshift plane for different X-ray fields in the 2–10 keV energy band. Right: log *N*–log *S* for the XXL-1000-AGN in the XXL-N field (blue circles) and in the XXL-S field (orange squares) as compared to other literature surveys (XXL Paper VI).

the diffuse light. Our spectral analysis shows that this emission likely originates from gas with a low-excitation parameter.

Globally, the stellar contribution to the ICL is about 2.3 × 10^9 years old even though the ICL is not currently forming a large number of stars. On the other hand, the contribution of the gas emission to the ICL in the optical is much greater than the stellar contribution in some regions, but the gas density is likely too low to form stars. These observations favour ram-pressure stripping, turbulent viscous stripping, or supernovae winds as the origin of the large amount of intracluster light. Since the cluster appears not to be in a major merging phase, we conclude that ram-pressure stripping is the most plausible process that generates the observed ICL sources.

AGNs in the XXL survey

X-ray extragalactic surveys are also ideal laboratories for the study of the evolution and clustering of AGN. Optimally, a combination of deep and wide surveys is necessary to create a complete picture of the population. Deep X-ray surveys provide the faint population at high redshift, while wide surveys provide the rare bright sources and the large-scale structure information. Nevertheless, very wide area surveys often lack the ancillary information available for modern deep surveys.

The XXL survey occupies the parameter space that lies between deep surveys and very wide area surveys, constituting a stepping stone between current deep fields and planned wide area surveys (Figure 5).

XXL-1000-AGN is our first point source catalogue. The sample is selected in the 2–10 keV energy band with the goal of providing an initial sizable sample useful for AGN studies (XXL Papers VI, XI, XII). The limiting flux is $F_{2-10\,keV} = 4.8\ 10^{-14}$ erg s^{-1} cm^{-2}. We use both public and proprietary datasets in the optical and near-infrared to identify the counterparts of the X-ray point-like sources by means of a likelihood ratio test, reaching 97.2 % identification rate. Using multi-wavelength data from the far ultra-violet to the mid infrared, we derive the median spectral energy distribution of AGN as a function of X-ray absorption. We improve upon the photometric redshift determination for AGN by applying a Random Forest classification trained to identify, for each object, the optimal photometric redshift category (passive, star-forming, starburst, AGN, quasar). In addition, we assign a probability to each source that indicates whether it might be a star or an outlier. The photometric redshift accuracy is 0.095 for the full XMM-XXL with 28 % catastrophic outliers estimated on a sample of 339 sources. We apply Bayesian analysis to model the X-ray spectra assuming a power-law model with the presence of an absorbing medium, finding no trend of photon index or hydrogen column density with redshift and a fraction of 26 % absorbed sources, consistent with the literature on bright sources.

The XXL-1000-AGN sample number counts extend the COSMOS log *N*–log *S* to higher fluxes (Figure 5); they are fully consistent with the Euclidean expectation and agree with previous deep (Chandra Deep Field South [CDFS] and COSMOS) and wide (Herschel-ATLAS) XMM-Newton surveys. We constrain the intrinsic luminosity function of AGN in the 2–10 keV energy band where the unabsorbed X-ray flux is estimated from the X-ray spectral fit up to $z = 3$. An application of the friends-of-friends algorithm, at 10 h^{-1} Mpc and 20 h^{-1} Mpc percolation radii, shows significant structures with 2–3 members and identifies a supercluster-sized structure at redshift 0.14.

In future publications we will expand the analysis to the full XXL catalogue, containing an unprecedented number of ~ 10^4 (X-ray) point-like 2–10 keV detected sources, and analysing the fully combined XMM pointings to reach maximum depth. A unique advantage of the XXL large statistical samples is the combined study of X-ray point-like sources and X-ray detected galaxy clusters, which will allow the study of AGN with respect to their environment and, *vice versa*, the study of the impact of AGN on clusters.

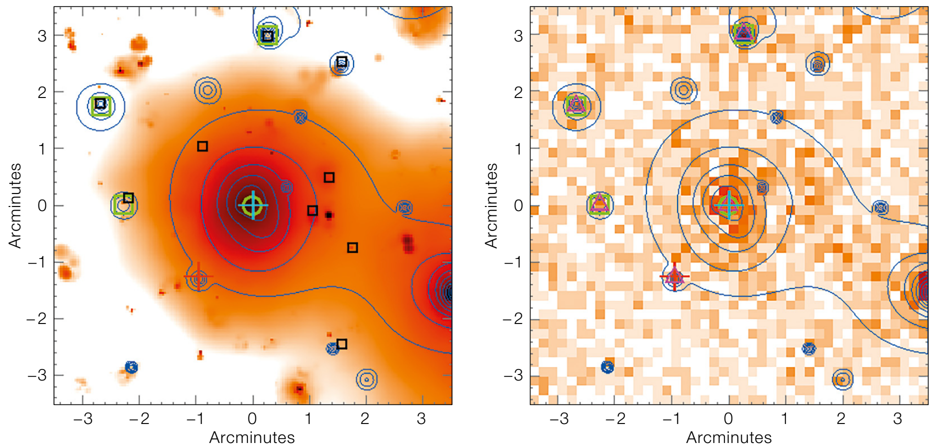

Figure 6. Left: Simulated X-ray emissivity map extracted from a 25 square degree by z = 0–3 light cone (OverWhelmingly Large Simulations [OWLS], Le Brun et al., 2014). Right: Same portion of the virtual sky transformed into an XMM image by the XXL simulator. All XMM characteristics are taken into account: point spread function (and its variation with energy), quantum efficiency, various background components and vignetting.

Prospects

The second phase of the XXL project is expected to end in 2018, with the publication of the complete cluster catalogue, including all data available from the multi-wavelength follow-up along with the selection functions. These will incorporate a thorough analysis of the impact of cluster shapes and AGN activity on the detection rates, which we will measure by means of *N*-body simulations performed under various physical hypotheses (Figure 6).

The final cosmological analysis of the full XXL cluster sample will involve a completely self-consistent treatment of the cluster evolution, selection function and cosmology. With some five times as many clusters (already some 450 clusters have been identified), we expect to provide a useful and stand-alone set of cosmological constraints. In addition to the traditional study of the *dn/dz* and *dn/dM/dz* counts, we have developed a method based on the modelling of the X-ray observable parameter space, that globally by-passes the intermediate phase of the (cosmologically dependent) cluster mass determination (Clerc et al., 2012; Pierre et al., 2016). We will also release the XXL multi-wavelength AGN catalogue, that is some 22 000 objects. The dataset, including spectroscopic follow-up, has a unique legacy value for cosmological and extragalactic environmental studies and will constitute a calibration resource for future surveys, like eRosita (all-sky, but at significantly lower sensitivity and resolution) and Euclid.

References

Clerc, N. et al. 2012, MNRAS, 423, 3561
Clerc, N. et al. 2012, MNRAS, 423, 3545
Driver, S. P. et al. 2016, MNRAS, 455, 3911
Hinshaw, G. et al. 2013, ApJS, 208, 19
Le Brun, V. et al. 2014, MNRAS, 441, 1270
Le Fèvre, O. et al. 2005, A&A, 439, 845
Guzzo, L. et al. 2014, A&A, 566, 108
Hinshaw, G. et al. 2013, ApJS, 208, 19

XXL Survey: I. Pierre, M. et al. 2016, A&A, 592, A1
XXL Survey: II. Pacaud, F. et al. 2016, A&A, 592, A2
XXL Survey: III. Giles, P. A. et al. 2016, A&A, 592, A3
XXL Survey: IV. Lieu, M. et al. 2016, A&A, 592, A4
XXL Survey: V. Mantz, A. B. et al. 2016, ApJ, 794, 157
XXL Survey: VI. Fotopoulou, S. et al. 2016, A&A, 592, A5
XXL Survey: VII. Pompei, E. et al. 2016, A&A, 592, A6
XXL Survey: VIII. Adami, C. et al. 2016, A&A, 592, A7
XXL Survey: IX. Baran, N. et al. 2016, A&A, 592, A8
XXL Survey: X. Ziparo, F. et al. 2016, A&A, 592, A9
XXL Survey: XI. Smolčić, V. et al. 2016, A&A, 592, A10
XXL Survey: XII. Koulouridis, E. et al. 2016, A&A, 592, A11
XXL Survey. XIII. Eckert, D. et al. 2016, A&A, 592, A12
XXL Survey XIV. Lidman, C. et al. 2016, PASA, 33, 1

Night-time observations with the New Technology Telescope at the La Silla Observatory.

Following two pages: VLT Survey Telescope (VST) composite *u*-, *g*- and *i*-band, large-field image (120 by 84 arcminutes) of the core of the nearby Fornax Galaxy Cluster. At a distance of about 19 Mpc, the Fornax cluster is a rich cluster (class 0) with more than 340 known members. The central brightest cluster galaxy, NGC 1399 can be seen to the north east, with the prominent barred spiral NGC 1365 to south west. See Release eso1612 for more details.